Universiteit
Leiden
The Netherlands

The cochlea depicted: radiological evaluation of cochlear morphology and the implanted cochlea

Jagt, M.A. van der

Citation
Jagt, M. A. van der. (2021, November 2). *The cochlea depicted: radiological evaluation of cochlear morphology and the implanted cochlea*. Retrieved from https://hdl.handle.net/1887/3238993

Version:	Publisher's Version
License:	Licence agreement concerning inclusion of doctoral thesis in the Institutional Repository of the University of Leiden
Downloaded from:	https://hdl.handle.net/1887/3238993

Note: To cite this publication please use the final published version (if applicable).

Chapter 2

Visualization of Human Inner Ear Anatomy with High Resolution Magnetic Resonance Imaging at 7 Tesla: initial clinical assessment

MA van der Jagt, WM Brink,
MJ Versluis, SCA Steens, JJ Briaire,
AG Webb, JHM Frijns, BM Verbist

Published in American Journal of Neuroradiology, 2014

Abstract

Background and purpose: In many centers, MRI of the inner ear and auditory pathway performed on 1.5 or 3 Tesla systems is part of the preoperative work-up of cochlear implant (CI) candidates. We investigated the applicability of clinical inner ear imaging at 7 Tesla MRI and compared the visibility of inner ear structures and nerves within the internal auditory canal (IAC) with images acquired at 3 Tesla.

Methods: 13 patients with sensorineural hearing loss (SNHL) eligible for cochlear implantation underwent examinations on 3 and 7 Tesla scanners. Two experienced head and neck radiologists evaluated the 52 inner ear data sets. A total of 24 anatomical structures of the inner ear and 1 overall score for image quality were assessed using a 4-point-grading scale for degree of visibility.

Results: The visibility of 11 out of the 24 anatomical structures was rated higher on the 7 Tesla images. There was no significant difference in the visibility of 13 anatomical structures and overall quality rating. A higher incidence of artifacts was observed in the 7 Tesla images.

Conclusions: The gain in SNR at 7T yielded a more detailed visualization of many anatomical structures, especially delicate ones, despite the challenges accompanying MRI at high magnetic field.

Introduction

Patients with sensorineural hearing loss (SNHL) suffer from malfunction of the inner ear, cochlear nerve or central auditory pathway. Treatment consists of amplification of sound or, in case of severe to profound SNHL, direct electrical stimulation of the cochlear nerve by a cochlear implant. MRI of patients with SNHL focuses on the integrity of the auditory pathways from the cochlea to the auditory cortex in the brain. In particular, the fluid-filled spaces of the labyrinth and internal auditory canal (IAC) and the cerebellopontine angle (CPA) are of interest because the most commonly identified pathologies that cause SNHL are found in these regions.[1–5]

One clear trend in the development of MRI systems has been the drive to higher magnetic field strengths.[6] For clinical inner ear scanning, MRI scanners with a magnetic field strength of 1.5 or 3 Tesla are routinely used. The relatively recent introduction of commercial 7 Tesla scanners potentially enables increased SNR resulting in more detailed imaging of anatomical structures. Concerning inner ear imaging, the visualization of delicate and small-sized inner ear structures might benefit from such high resolution imaging. This may yield new opportunities for obtaining normative measurements and for evaluating pathological alterations within the inner ear or associated nerves. Such detailed anatomical description has gained particular interest for assessment of cochlear implant candidates, since it gives decisive information on implantation feasibility, possible surgical risks, and choice of implant device. As such it would aid in patient-specific preoperative planning of cochlear implantation and could provide valuable information for individualized assessment of insertion.

Transition from a conventional 3 Tesla scanner to a stronger 7 Tesla scanner is challenging, however, due to technical complexities accompanying higher magnetic field strength.[6] One of these technical complexities is the increased inhomogeneity of the static (B_0) and radiofrequency (B_1) field, typically featuring areas of low B_1 close to the temporal lobes. The B_0 inhomogeneities are caused primarily by the susceptibility difference between inner ear fluids and the surrounding bone, and the B_1 inhomogeneities by the elliptical shape of the head. Both of these effects can result in loss of signal in the inner ear region as previously described by Takahara et al and Van Egmond et al.[7–9] Additionally, the specific absorption rate, for which regulatory safety limits are defined, scales approximately quadratic with field strength, ultimately limiting the imaging speed at high fields in vivo. Recently, we introduced geometrically tailored dielectric pads to locally tailor the B_1 distribution. This improved contrast homogeneity and transmit efficiency in the region of the inner ear without increasing the specific absorption rate, which contributed to the development of a high resolution imaging protocol at 7 Tesla.[10]

The aim of this study was (1) to investigate the applicability of clinical inner ear imaging at 7 Tesla MRI and (2) to compare the visibility of inner ear structures and nerves within the internal auditory canal (IAC) with images acquired at 3 Tesla.

Materials and methods

Patients

This prospective study was approved by the hospital institutional review board (P07.096). Patients with SNHL, eligible for cochlear implantation and referred for 3 Tesla imaging between December 2012 and May 2013, were asked to participate in the study. Exclusion criteria were age under 18 years and contraindications for exposure to the magnetic field. Seventeen candidates for cochlear implantation were enrolled in the study; 9 females and 8 males between 27 and 78 years of age. Etiology and duration of hearing loss are described in Table 1. All patients underwent an MRI examination at 3 Tesla as part of the standard work-up for cochlear implantation. After obtaining written informed consent, sixteen patients underwent an examination at 7 Tesla; one patient was excluded due to intracranial foreign body of unknown composition. Three other patients were excluded after the scanning procedure due to the following reasons: scans of two patients were incomplete due to premature termination of the scanning procedure due to an unspecified technical defect and the scanning procedure of one patient had to be aborted due to claustrophobia. After the procedure patients were asked if they had suffered from dizziness, as this is a frequently reported but temporary side effect of scanning at 7 Tesla.

Table 1. Demographic details of studied patients (N=17)

		N
Sex		
	Male	8
	Female	9
Pathologic imaging reportings		
	Cochlea malformation	1*
	Hypoplasia acoustic nerve	1*
	Fenestral otosclerosis	1
	Labyrinthitis ossificans	1
	None	14
Etiology		
Congenital		
	Pendred syndrome	1
	of unknown origin	5
Acquired		
	Sudden deafness	2
	MIDD**	1
	Otosclerosis	2
	Rubella infection	2
Unknown		4
		Mean (years)
Duration of deafness		23.2

* Same patient

Imaging technique

All patients underwent examination on a Philips Achieva or Ingenia 3 Tesla system (Philips Healthcare, Best, The Netherlands) as part of the standard preoperative work-up. The following scan parameters were used for the T_2-weighted TSE sequence: field-of-view 130 x 130 x 24 mm, 0.6 mm^3 isotropic voxels, TR/TE/TSE factor = 2400ms/200ms/73 and 80 slices, resulting in an acquisition time of approximately 6 minutes. In addition, all patients were scanned on a Philips Achieva 7 Tesla system (Philips Healthcare, Best, The Netherlands) as described by Brink et al, using a quadrature transmit and 32 channel receive coil (Nova Medical, Wilmington, MA).[10] To improve contrast homogeneity and transmit efficiency two gender-specific high permittivity pads, containing a suspension of barium titanate and deuterated water, were positioned next to both ears.[10] High resolution T_2-weighted images were acquired using the following parameters: field-of-view 180 x 180 x 24 mm, 0.3 mm^3 isotropic voxels, TR/TE/TSE factor = 3000 ms/200 ms/69, tip angle/refocusing angle = 90°/135°, parallel imaging reduction factor = 2.5 x 1.5 and 160 slices. This resulted in an acquisition time of approximately 10 minutes.

Image analysis

The high resolution T_2-weighted images acquired at both the 3 and 7 Tesla scanners were transferred to OsiriX DICOM viewer.[11] The images were anonymized and presented in randomized order. Evaluation was performed by two head and neck radiologists with 5 and 13 years of experience, respectively. A total of 24 anatomical structures of the inner ear were assessed using a 4-point-grading scale for degree of visibility for diagnostic evaluation: 1 = not assessable, 2 = poor, 3 = adequate, 4 = excellent. The structures selected were those most relevant for cochlear implantation. In addition, an overall score for diagnostic image quality was granted: 1 = not diagnostic, 2 = poor, 3 = adequate, 4 = excellent. Both ears were evaluated separately. Subsequently the scores of the two ears and two observers were averaged and normalized into a parameter between 0 and 1. An overview of the anatomical structures and their difference in rating is shown in Figure 4. The numbers I, II and III refer to the basal, mid and apical turn, respectively.

Statistical analysis

Statistical analysis was performed using SPSS (IBM Corp Released 2011. IBM Statistics for Windows, Version 20.0. Armonk, NY: IBM Corp). In order to study the influence of observed asymmetrical signal intensity between the right and left inner ear on the 7 Tesla images, a linear mixed model was performed. Statistical differences per anatomical structure between the 3 and 7 Tesla scanner were determined using a Wilcoxon signed rank test. The inter-rater variability was determined by the Kappa coefficient of Cohen. All tests were two-tailed and $P < 0.05$ was considered to indicate a statistically significant difference.

Results

Twenty six inner ears of 13 patients were available for image analysis. The occasionally observed asymmetrical signal intensity on some of the 7 Tesla images did not result in a significant different rating of the right and left inner ear (p=0.215). Therefore no distinction between inner ear sides was used for analysis. As 24 anatomical structures per inner ear were evaluated on T_2-weighted images acquired on 3 and 7 Tesla scanners plus an additional score for overall image quality, this resulted in 2600 ratings applied by the two observers together. The ratings were averaged over ear and observer, leaving 650 ratings for statistical analysis. The visibility of 11 out of the 24 anatomical structures was rated higher on the 7 Tesla images. None of the anatomical structures were better depicted on the 3 Tesla images. There was no significant difference in the visibility of 13 anatomical structures and the overall diagnostic image quality rating. The inter-observer agreement was moderate with a κ-value of 0.55. None of the patients reported excessive or extended dizziness during or after the scan procedure.

Cochlea

Figure 1 shows the cochlea on an axial cross-section image, clearly illustrating the improved resolution of the 7 Tesla image contributing to a more detailed depiction of the inner ear anatomy. Evaluated cochlear structures include the scala vestibuli, scala tympani, scala media, osseous spiral lamina and interscalar septa. All structures were evaluated separately for each cochlear turn. Significant differences in favor of the 7 Tesla images were found for the scala tympani and vestibuli in the 2nd and 3rd turn, with a mean difference of 0.13 (p = 0.023) and 0.31 (p = 0.023) for the 2nd turn and 0.14 (p = 0.002) and 0.31 (p = 0.002) for the 3rd turn. The scala media in the first turn could be distinguished in 7 out of 52 ratings on the 7 Tesla images, but in none of the inner ears on the 3 Tesla images. Visualization of these distinguished scala medias were 6 times evaluated as ‘poor’ and one time as ‘adequate’. The resulting score difference of 0.05 was not significant (p = 0.066). In the second turn, the scala media was visible in 21 inner ears on the 7 Tesla images, compared to none on the 3 Tesla images. The degree of visibility of these structures was rated ‘poor’ in 16 cases, ‘adequate’ in 3 cases and ‘very good’ in 2 cases. The score difference of 0.18 was significant for this turn (p = 0.005). In the second and third turn, the depiction of the osseous spiral lamina was better on the 7 Tesla images, resulting in a sharp delineation of the scala tympani and vestibule (p = 0,006 for the second turn and p = 0.001 for the third turn). The visibility of the interscalar septum between the second and third turn also significantly benefits from high resolution imaging at 7 Tesla (p = 0.003).

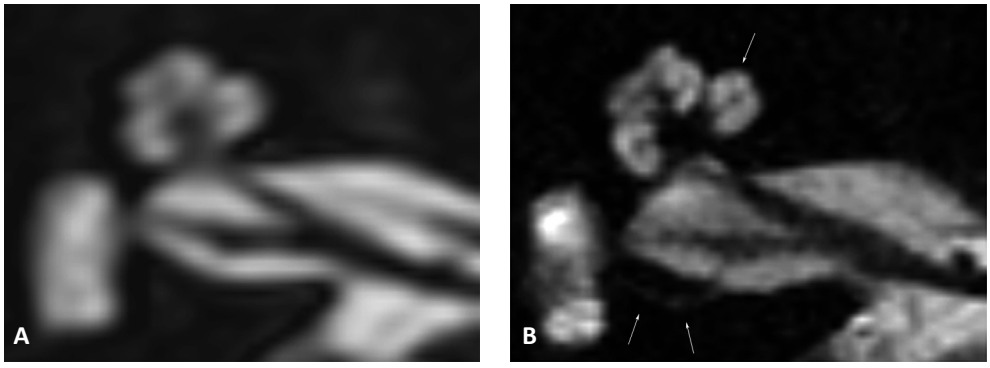

Figure 1: Axial cross-section of a right inner ear, rendered at 3 Tesla (A) and 7 Tesla (B); improved discrimination of the intra cochlear structures and compartments is shown. Also sharper delineation of the nerves in the internal auditory canal is demonstrated. The single arrow indicates the scala media at the first turn. The double arrows indicate the superior ampullary nerve.

Internal auditory canal

Statistical differences in visualization of the facial ($p = 0.259$), superior ($p = 0.131$) and inferior vestibular ($p = 0.242$) and cochlear nerve ($p = 0.151$) through the internal auditory canal could not be demonstrated. On the 3 Tesla images, the intermediate nerve was observed 5 out of 52 times, compared to 31 times on the 7 Tesla images. On the 7 Tesla images the visibility of the intermediate nerve was evaluated as 'poor' in 14 cases, 'adequate' in 8 cases and 'excellent' in 9 cases. This resulted in a significant difference of 0.32 ($p = 0.002$). An example of the clear depiction of an intermediate nerve is shown in Figure 2. Also a sharper delineation of the other neural structures is obtained. The superior ampullary nerve is indicated in Figure 1B by two white arrows. This small neural structure is not regularly visualized on 3 Tesla scans. In this study it was observed 10 out of 52 times on the 3 Tesla scans; 7 times 'poor' and 3 times 'adequate', compared to 28 times on the 7 Tesla scans; 11 times 'poor', 6 times 'adequate' and 11 times 'excellent'. This resulted in a significant difference of 0.28 ($p = 0.009$).

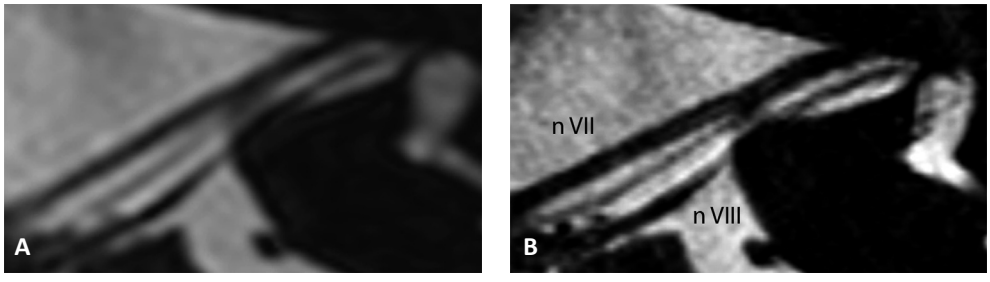

Figure 2: Axial cross-section along the course of the facial nerve of a left inner ear, rendered at 3 Tesla (A) and 7 Tesla (B). A sharp delineation of the neural structures and clear depiction of the intermediate nerve between n VII and n VIII is demonstrated at the 7 Tesla image.

The visualization of the falciform crest was significantly improved on the 7 Tesla images; it was identified in 47 out of 52 readings on the 7 Tesla images, compared to 41 readings on the 3 Tesla images. This led to a score difference of 0.25 ($p = 0.022$). Bill's bar was only occasionally observed at either magnetic field strength.

Cochlear and vestibular aqueducts

Visualization of the vestibular aqueduct (VA) and cochlear aqueduct (CA) did not differ significantly among the 3 and 7 Tesla images. A score difference of 0.16 ($p = 0.107$) of the VA and 0.01 ($p = 0.836$) of the CA were found.

Artifacts

A higher incidence of image artifacts was observed in the 7 Tesla images; 9 out of the 13 scans versus none of the 3 Tesla scans. These artifacts include motion artifacts likely due to the prolonged scan duration compared to 3T. Also off-resonance effects due to the increased B_0 inhomogeneities causing signal loss and stripe-like artifacts likely due to B_1-inhomogeneities were observed. An example of their appearances is shown in Figure 3.

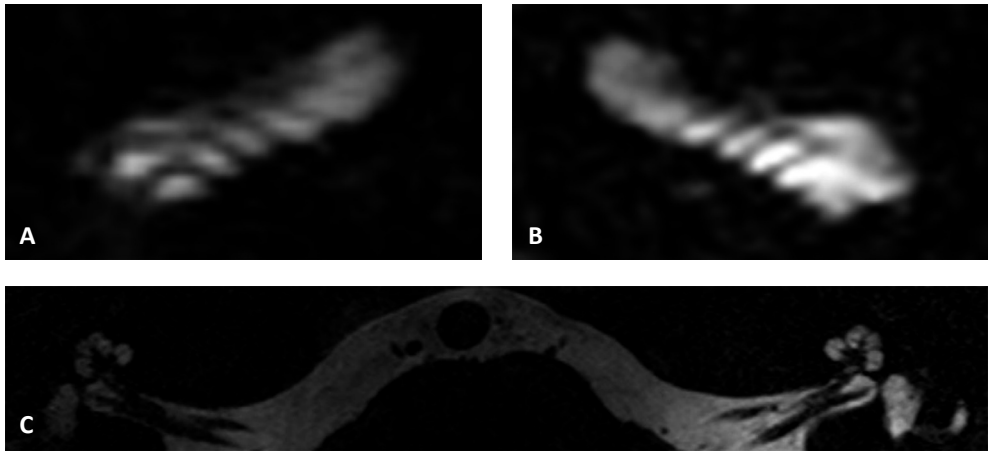

Figure 3: 7 Tesla images showing stripe like-artifacts at the level of the first turn of a right (A) and left (B) cochlea of 2 different patients, disturbing the quality of its representation and impeding the distinction of the scala vestibuli and tympani. Asymmetrical signal intensity was observed occasionally (C).

Overall image quality

Image quality can be expressed as either the mean of scores per magnetic field strength or the actual applied score for image quality. Firstly we calculated the sum of scores, separately for each magnetic field strength. Comparison of these values resulted in a significant difference of 0.11 per anatomical structure in favor of the 7 Tesla scanner ($p << 0.001$). Secondly, the score for overall image quality as rated directly was analyzed. This score for overall image quality was applied in the context of diagnostic value, meaning distortion of

the image quality by artifacts was taken into account. Comparing these scores did not show a significant difference between the two field strengths ($p = 0.631$).

An overview of all the described outcomes is presented in Figure 4.

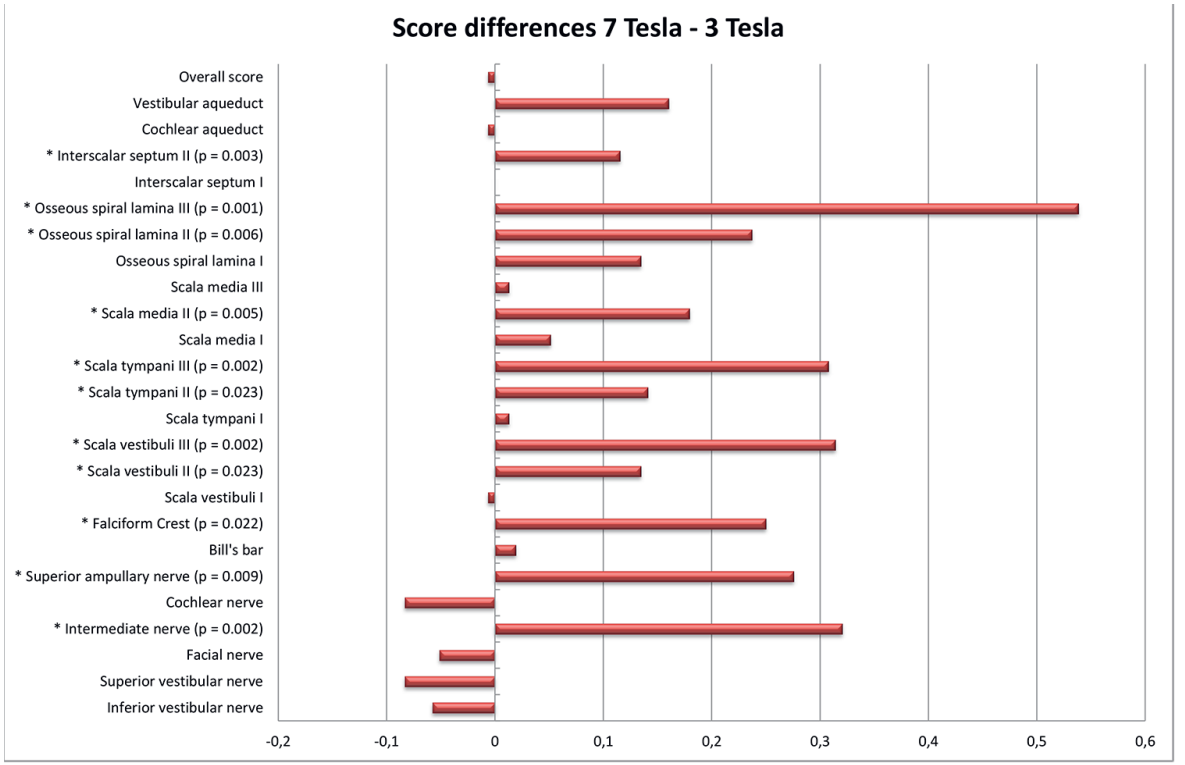

Figure 4: Mean differences in scoring of anatomical structures depicted at 3 and 7 Tesla images. The red bars on the right side of the 0-line indicate differences in favor of the 7 Tesla images. The bars on the left side indicate differences in favor of the 3 Tesla images. The structures showing significant differences are marked with an asterisk on the left and p-values are mentioned if significant.

Discussion

7 Tesla MR imaging of the inner ear was successfully performed in patients with profound SNHL eligible for cochlear implantation. Comparison with 3 Tesla images demonstrated improved visualization of a large number of anatomical structures of the inner ear and internal auditory canal with high resolution 7 Tesla imaging and emphasized the potential of clinical imaging at 7 Tesla.

Regarding the cochlear structures, the benefit of increased SNR was most pronounced for visualization of the microstructures of the 2nd and 3rd turn. The accurate distinction of the different turns and compartments is essential to accurately diagnose and localize pathologies and to support surgical planning. One specific development over the last years that has emphasized the role of radiological evaluation of cochlear implant candidates is the expanded criteria for cochlear implant recipients. A malformed cochlea is no longer an absolute contraindication for implantation, which is important as up to 20% of the patients with SNHL show some degree of inner ear malformation.[12] However, when a malformation is present, the surgical procedure carries a higher risk for complications such as cerebrospinal fluid gusher, and often a different surgical approach and electrode type need to be chosen to ensure a good outcome.[13] These considerations require precise preoperative planning, and an increase in anatomical information as achieved with 7 Tesla could be beneficial in such patients. Another example where an increase in anatomical information could be extremely relevant includes patients with obliterated cochleas. This fibrotic or osseous obliteration of the cochlear lumen is usually caused by meningitis-induced labyrinthitis. When parts of the cochlea are not patent, a different surgical approach should be followed with, in some cases, the use of a split array electrode.[14] This device was developed to maximize the coverage of spiral ganglion cells by inserting two separate arrays through different cochleostomies. To precisely guide this procedure, comprehensive details of the cochlea anatomy are required. For electro-acoustic stimulation (EAS), cochlear trauma needs to be minimized and preoperative delineation of the cochlear anatomy should be as accurate as possible. In addition, gain in detailed anatomical information of the cochlea enables further research on morphological characteristics, their influence on electrode position and its relation to CI recipients' performance.[15,16]

At the location of the internal auditory canal, smaller nerve branches such as the superior ampullary nerve and the intermediate nerve were in general better depicted at 7 Tesla. The fact that larger neural structures did not benefit from the increased resolution at 7 Tesla can be explained by (1) motion artifacts, (2) off-resonance and stripe-like artifacts and (3) the scoring system. The internal auditory canal where these structures are housed was particularly vulnerable to patient-induced motion artifacts. It was observed that the neural structures in the internal auditory canal were more frequently affected than the cochlear

structures when motion of the head took place during the scan procedure. An explanation for this observation is not well defined yet, but one can realistically hypothesize a combination of the direction of the motion and the dimensions of the IAC that makes it more vulnerable. Scanner-related artifacts such as the stripe-like artifacts and off-resonance were only pronounced at higher field strength, as might be expected from the implicit larger absolute change in resonance frequency. Another contributing factor might have been the chosen 4-point grading scale. In the majority of cases, the visibility of nerves were rated 'excellent', based on delineation of the neural structures in both the 3 and 7 Tesla images. Consequently a distinction in visualization between the 2 scanners is hardly detectable and decisive for evaluation was the presence of artifacts. Yet, although not evaluated systematically one observer reported more confident assessment on cochlear nerve hypoplasia at 7 Tesla.

With respect to the clinical relevance, it is important to realize that many etiologies causing SNHL cannot be seen *in vivo* with current techniques. By increasing SNR and resolution, however, it is expected that more anatomical changes related to SNHL can be demonstrated. By showing the capability of 7 Tesla MRI to visualize anatomical structures such as the distinguished scalas of the 2nd and 3rd turn, scala media, intermediate nerve and superior vestibular nerve, a first step towards that expectation has been made. When etiologies are known, treatment and prognosis can be tailored more accurately. Improved image quality does however come with a number of drawbacks and limitations. An example of such a limitation is the prolonged scan duration. In our study scan duration was prolonged from 6 to 10 minutes. This prolongation together with the lack of communication possibilities for this specific patient population caused an increased susceptibility to subject-induced artifacts, and therefore the use of communicative visual signaling during scanning is recommended. Additionally, the likelihood of motion artifacts could be reduced by shortening scan duration through reduced FOV imaging techniques.[17] Another important issue is the presence of possible side effects during 7 Tesla examinations. Previous research reports a slightly higher incidence of dizziness than at 3 Tesla, discomfort from the gradient noise and a metallic taste.[18–20] Nevertheless, these side effects are widely accepted and in general 7 Tesla examinations are tolerated well. In our study population none of the patients mentioned excessive discomfort during the scan procedure.

Another limitation of our study is the difference in background of the observers. One observer normally evaluates MR images acquired at 3 Tesla, whereas the second observer normally evaluates MR images acquired at 1.5 Tesla only. This may have resulted in overvaluation of the 3 Tesla images by the second observer, thereby diminishing the difference between the 3 and 7 Tesla images and decreasing the a κ-value.

Conclusion

We report progress toward the use of 7 Tesla MRI for inner ear scanning in a clinical setting. The gain in SNR resulted in a more detailed visualization of a large number of relevant anatomical structures despite the remaining difficulties accompanying high magnetic field imaging. The findings of this study are encouraging to continue research on technical adjustments to push the limits of 7 Tesla MRI to reach its full potential and make it suitable for clinical applications.

References

1. Verbist BM. Imaging of sensorineural hearing loss: a pattern-based approach to diseases of the inner ear and cerebellopontine angle. *Insights Imaging*. 2012;3(2):139–53.
2. Casselman JW. Diagnostic imaging in clinical neuro-otology. *Curr Opin Neurol*. 2002;15(1):23–30.
3. St Martin MB, Hirsch BE. Imaging of hearing loss. *Otolaryngol Clin North Am*. 2008;41(1):157–78.
4. Mohan S, Hoeffner E, Bigelow DC, Loevner L a. Applications of magnetic resonance imaging in adult temporal bone disorders. *Magn Reson Imaging Clin N Am*. 2012;20(3):545–72.
5. Davidson HC. Imaging evaluation of sensorineural hearing loss. *Semin Ultrasound CT MR*. 2001;22(3):229–49.
6. Robitaille P, Berliner L. *Ultra high-field magnetic resonance imaging*.; 2006.
7. Sled JG, Pike GB. Standing-wave and RF penetration artifacts caused by elliptic geometry: an electrodynamic analysis of MRI. *IEEE Trans Med Imaging*. 1998;17(4):653–62.
8. Takahara T, Hoogduin H, Visser F, Naganawa S, Kwee T, Luijten P. Imaging of the Inner Ear at 7T : Initial Results. In: *Proceedings of the 18th Annual Meeting of ISMRM. Stockholm, Sweden; 2010:4448.*Vol 17.
9. Van Egmond SL, Visser F, Pameijer F a, Grolman W. Ex Vivo and In Vivo Imaging of the Inner Ear at 7 Tesla MRI. *Otol Neurotol*. 2014:1–5.
10. Brink WM, van der Jagt AMA, Versluis MJ, Verbist BM, Webb AG. High Permittivity Dielectric Pads Improve High Spatial Resolution Magnetic Resonance Imaging of the Inner Ear at 7 T. *Invest Radiol*. 2014;00(00):1–7.
11. Rosset A, Spadola L, Ratib O. OsiriX: an open-source software for navigating in multidimensional DICOM images. *J Digit Imaging*. 2004;17(3):205–16.
12. Sennaroglu L. Cochlear implantation in inner ear malformations--a review article. *Cochlear Implants Int*. 2010;11:4–41.
13. Sennaroglu L, Sarac S, Ergin T. Surgical results of cochlear implantation in malformed cochlea. *Otol Neurotol*. 2006;27:615–623.
14. Millar D a, Hillman T a, Shelton C. Implantation of the ossified cochlea: management with the split electrode array. *Laryngoscope*. 2005;115(12):2155–60.
15. Van der Marel KS, Briaire JJ, Wolterbeek R, Snel-Bongers J, Verbist BM, Frijns JHM. Diversity in Cochlear Morphology and Its Influence on Cochlear Implant Electrode Position. *Ear Hear*. 2013:1–12.
16. Holden LK, Finley CC, Firszt JB, et al. Factors affecting open-set word recognition in adults with cochlear implants. *Ear Hear*. 2013;34(3):342–60.
17. Wargo CJ, Moore J, Gore JC. A comparison and evaluation of reduced-FOV methods for multi-slice 7T human imaging. *Magn Reson Imaging*. 2013;31(8):1349–59.
18. Heilmaier C, Theysohn JM, Maderwald S, Kraff O, Ladd ME, Ladd SC. A large-scale study on subjective perception of discomfort during 7 and 1.5 T MRI examinations. *Bioelectromagnetics*. 2011;32:610–9.
19. Theysohn JM, Maderwald S, Kraff O, Moenninghoff C, Ladd ME, Ladd SC. Subjective acceptance of 7 Tesla MRI for human imaging. *MAGMA*. 2008;21:63–72.

20. Versluis MJ, Teeuwisse WM, Kan HE, van Buchem M a, Webb AG, van Osch MJ. Subject tolerance of 7 T MRI examinations. *J Magn Reson Imaging*. 2013;38:722–5.